

Stabilising A Vertically Driven Inverted Pendulum

J. J. Aguilar,¹ C. Marcotte,¹ G. Lee,¹ and B. Suri¹

*School of Physics, Georgia Institute of Technology, Atlanta, Georgia 30332,
USA*

(Dated: 16 December 2011)

In this article we discuss the preliminary results of stabilising a vertically driven pendulum. Following the brief introduction on the importance of this ‘toy’ problem, we give an account of the experimental set up. We then explain the parameter extraction from the experimental data which form a crucial part of our quantitative study. We also find the stability boundary for a small range of driving frequencies and amplitudes and match it with the simulation. We finally present a qualitative description of stabilising the double pendulum.

I. INTRODUCTION

Stabilising an inverted pendulum is a problem that has been studied for academic as well as for practical reasons. It is one of the few nonlinear problems where considerable analytical progress has been made to gain insight into the dynamics of the system^{1,2}. From a practical standpoint, the problem of ‘bottom light - top heavy’ configuration is ever present in nature and finds application in control theory - which in turn has penetrated into fields like Engineering, Physiology³, Neurology⁴, just to name a few.

In this article we first briefly introduce the theory behind the mathematical formulation of the problem. We then describe the experimental set up. The details of the choice of equipment was relegated to the appendices.

In the section following set-up, we present our results, primarily concerning parameter estimation, stability boundary, and small oscillations. We conclude by a short mention of stabilising a double pendulum. In the appendices we include information about tracking the pendulum and experimental constraints.

II. THEORY

Consider a pendulum with a mass m attached to a massless rod of length l (figure 1). The pivot of the pendulum is fixed to an oscillator that can be driven in the vertical direction. The displacement of the pivot at any instant be $y(t)$. The system has only one independent variable θ which measures the angular displacement of the pendulum from the vertical position. The Lagrangian \mathcal{L} of the

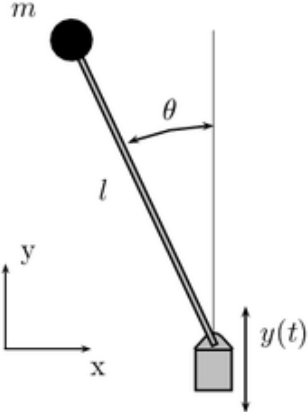


FIG. 1. Schematic Diagram of a vertically Driven Inverted Pendulum

system is given by equation 1. The Euler-Lagrange equation of motion for θ is given by equation 2.

$$\mathcal{L} = \frac{m}{2}(\ell^2\dot{\theta}^2 + \dot{y}^2 + 2\ell\dot{y}\dot{\theta}\sin\theta) - mg[y(t) + \ell\cos(\theta)] \quad (1)$$

$$\ddot{\theta} = \sin\theta\left(\frac{g}{\ell} + \ddot{y}(t)\right) \quad (2)$$

Till now we have assumed that the system is conservative, i.e. there is no loss of energy

due to damping. To include a damping term in the equation of motion (eq 2) we consider two possible sources of damping: firstly, the damping due to viscous drag and then damping due to a constant frictional ‘torque’ at the pivot. Due to the small physical dimensions of the pendulum and the ‘low’ speeds, we assume that the damping is primarily due to friction at the pivot. We hence include a damping term into the equation of motion(eq

2) which yields the complete evolution equation (eq 3).

$$\ddot{\theta} = \sin\theta\left(\frac{g}{\ell} + \ddot{y}(t)\right) - \Gamma(\dot{\theta}) \quad (3)$$

If the pendulum is not driven ($\ddot{y}(t) = 0$) then it stabilises about $\theta = \pi$. For small disturbances about $\theta = \pi$ it oscillates with a decaying amplitude and with frequency $\omega_0^2 = \frac{g}{l}$. The next task is to interpret the role of Γ in the amplitude decay of the system. If we assume that the un-driven pendulum started from an extremum $-\theta_0$ ($\theta_0 \ll 1$) about $\theta = \pi$, it suffers a decrease in angular displacement at the next extremum by $\delta\theta$ (i.e. $\theta_f = \theta_0 - \delta\theta_0$). The work done by the friction during this time must be equal to the loss in the potential energy. This can be easily seen by multiplying the evolution equation (eq 3) with $\dot{\theta}$ and integrating over half a cycle. This gives

$$\Gamma = \frac{2\pi^2\delta\theta_0}{T^2} \quad (4)$$

Resuming our discussion on the driven pendulum, the form of driving is something we have not discussed. Previous work shows that sinusoidal and triangular⁵ driving waveforms have been analytically studied and the results are very similar. In our experiment we use sinusoidal waveform wave form ($y(t) = A\sin ft$). These parameters can be non dimensionalised as $\epsilon = \frac{A\omega_0^2}{g}$ and $\Omega = \frac{f}{f_0}$. The preliminary goal would be to identify the sta-

bility boundary in the ϵ, Ω space. Previous work¹ shows that the inverted state is stabilised so long as the driving amplitude and frequency fall within the curves

$$\epsilon = \frac{\sqrt{2}}{\Omega} \quad \text{and} \quad \epsilon = 0.45 + \frac{1.799}{\Omega^2} \quad (5)$$

III. EXPERIMENTAL SET-UP

In this section we briefly describe the set-up we use in this experiment. The minor details, if any, would be given in the appendices. The pendulum is a 3.1 cm short Aluminium beam, pivoted to a shaft with the help of a skate board bearing. The shaft is then attached to a base which is fixed to a shaker. A signal generator sends a signal via an amplifier to a speaker, which then converts the signal into a mechanical oscillations. These oscillations are transferred to a horizontal base with the help of a hydraulic mechanicsm.

For tracking the pendulum position, we paint the pendulum and the background black and mark the pivot and the pendulum tip with a white dot. For low speed experiments, like the spin down one, we use a Point Grey highspeed camera, capable of 200fps which transfers images to a computer using firewire. The computer uses Labview software to track the position of the pointers (in pixel units). For experiments with faster moving pendulum, like ones where the

pendulum makes a full rotation, we use a MotionXtra camera at 1000fps. The data is saved as a video from which we extract the traker positions using Matlab image processing.

IV. RESULTS

The decay profile of the pendulum is shown in figure 2.

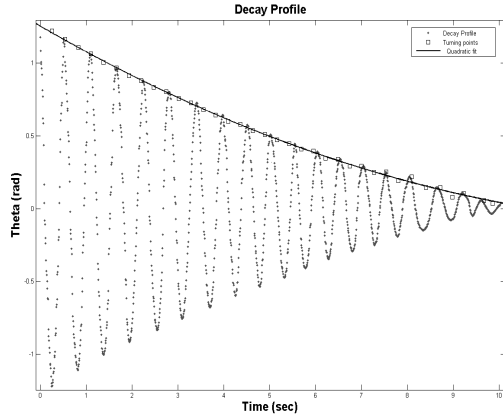


FIG. 2. Amplitude decay of the pendulum

An FFT on the data gives the natural frequency of the pendulum as 1.793 Hz (fig 3). The turning points are then fit to a quadratic curve with the quadratic (β) and linear coefficients(α) being 0.006 and 0.18 respectively. This shows that the decay is predominantly linear, in accordance with our constant friction model. From the frequency of oscillation and the decay profile slope (α), the Damping Parameter Γ (6) is estimated to

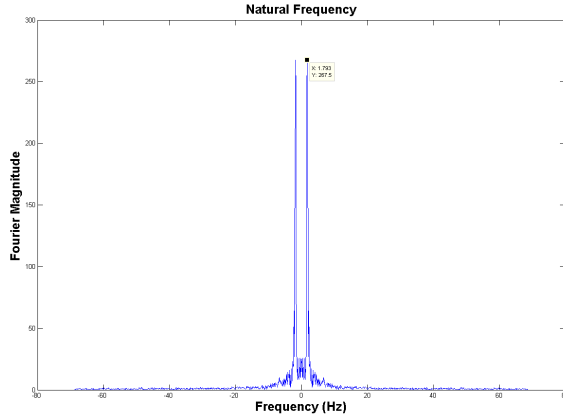


FIG. 3. Frequency of natural oscillations

have a value 3.1.

$$\Gamma = \frac{\pi^2}{T} \frac{(2\delta\theta_0)}{T} = \frac{\pi^2\alpha}{T} \quad (6)$$

To test the accuracy of these parameters, we integrate the equation of motion 3, with $\ddot{y} = 0$, and plot it against the experimental data. The initial conditions are obtained from experimental data. Since the amplitude of the oscillations is not small, as was supposed in the derivation of eq 6, the value of Γ calculated from eq 4 does not give a close fit. In fact, using a frequency 1.87 Hz and $\Gamma = 2.5$ we get a good agreement between experiment and simulation (fig 4).

We then analyse the stability boundary of the inverted pendulum in the ϵ, Ω parameter space. For a given frequency we determine the amplitude of vibrations necessary for the pendulum to stabilise in the vertical position, starting from an initial position close to $\theta = 0$. Since the experimental setup constrained

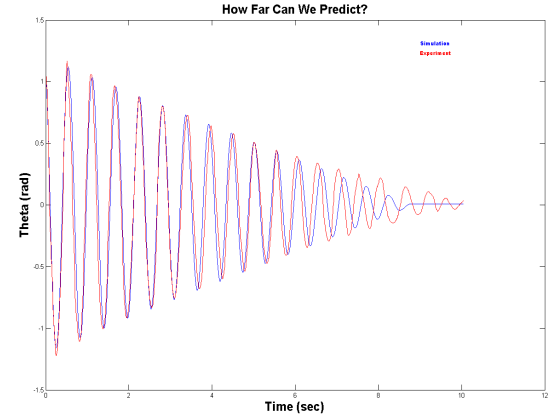


FIG. 4. Comparison between simulation and Experimental data

the range of amplitudes we could explore, the data is obtained for a short range of frequencies (fig 5). Non dimensionalising and comparing these to the simulated boundaries (eq 5) shows a very good agreement (fig 6).

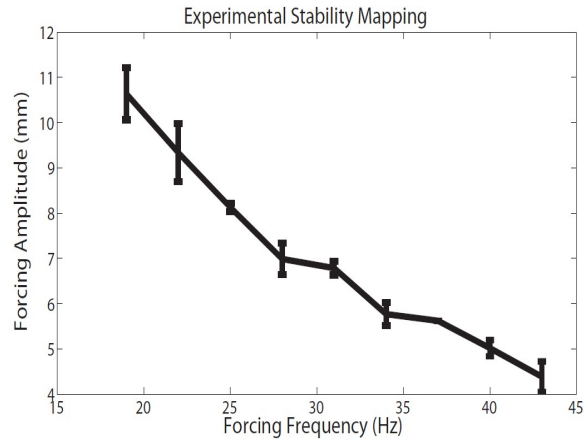


FIG. 5. Experimentally determined stability boundary

Finally, we measure the frequency of small oscillations about the stabilised inverted position. We find a positive correlation between

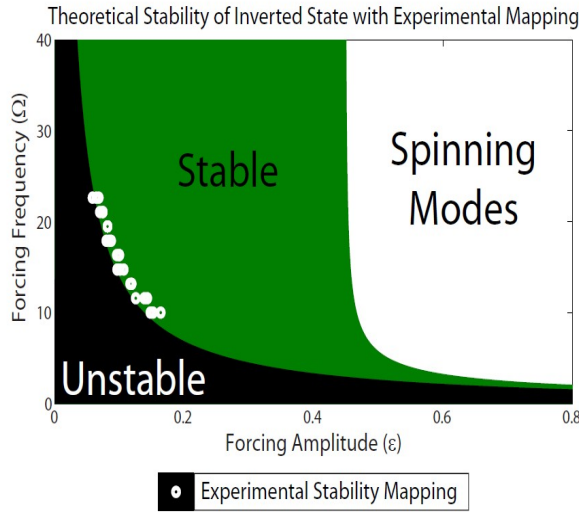


FIG. 6. Stability boundary comparison

the driving amplitude and the frequency of oscillations (fig 7). However, quantitative analysis was not possible due to the limited range of amplitudes that could be explored using the equipment available.

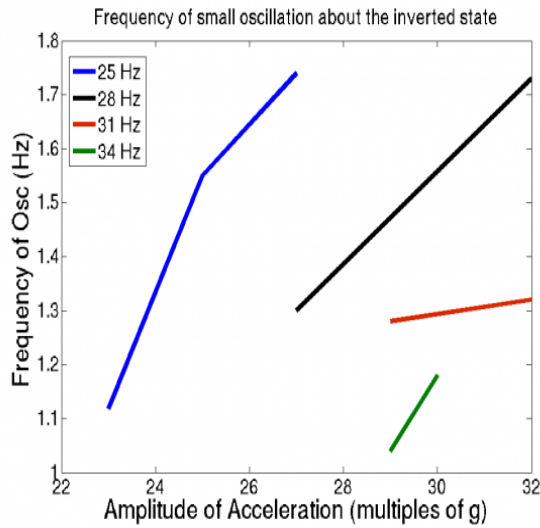


FIG. 7. Frequency of small oscillations

V. DOUBLE PENDULUM

Before we conclude, we would like to present a time series plot (fig 8) from the double pendulum stabilisation. The pendulum constructed using two 4cm long legos. Quantitative analysis was not performed on this set up, but we have achieved stabilisation of the double pendulum. The following image shows that both the pendula stabilise around $\theta = 0$, making small oscillations about the inverted state.

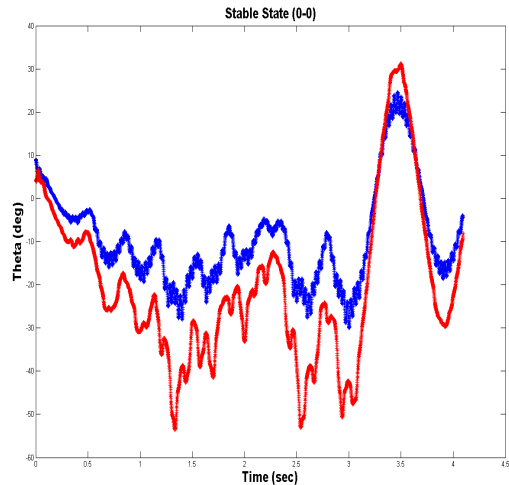


FIG. 8. Stabilisation of double pendulum

VI. CONCLUSIONS

In our experimental study we have successfully stabilised the vertically driven inverted pendulum, obtaining all the parameters that govern the evolution of the system. We have successfully explored a small portion

of the parameter space for stability boundary. We have found that there is a positive correlation between the frequency of small oscillations about the inverted position and the amplitude of forcing. Finally, we have successfully stabilised a double pendulum, though quantitative analysis was not possible. Future work may include predicting the evolution of the pendulum by obtaining initial conditions from the experiment and integrating the equations describing the model (eq 3). Also, a more sophisticated set up, with a more capable shaker, can help exploring larger regions in parameter space for stability boundaries. A quantitative analysis of the double pendulum is right next in line, and a possible extension to higher number of pendula.

Appendix A: Experimental Constraints

The primary glitch we encountered was with a ‘longer’ (6 cm) pendulum we started the experiment with. This pendulum was mounted using two skate-board bearings on an axle. The axle would bend a little when fixed to the shaker, and also because one of the bearings was worn out we observed fixed points that were not vertically aligned with gravity (fig 9). For small oscillations the pendulum would toggle rapidly as if it had fallen

in a groove. To correct for this we removed one of the bearings. This rectified the bent axle too. Another vital constraint was the

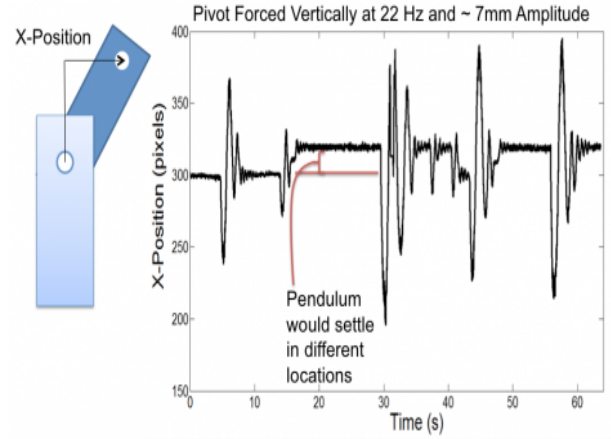


FIG. 9. Pendulum falling into a groove

amplitude of shaking. The shaker could force oscillations of amplitudes about 12mm. Beyond this there would be a ‘knocking’ sound, which meant the airbearing was over shooting its limits. To work within the limits of the shaker we needed to shorten (to 3 cm) the length of the pendulum, since it would require smaller oscillations to stabilise it.

Appendix B: Tracking

For low speed experiments, like the one with small oscillations about the vertical position or the spin down experiment, we use a Point Grey camera capable of capturing images at 200 fps. The data is analysed in parallel using Labview and the tracker position is stored directly as pixels. However, when

the pendulum moves at greater speeds, the marker position is lost and we resort to using MotionXtra camera at 1000 fps. The data is stored as a single video file from which we extract the images. Once the images are obtained, we convert all of them to binary data files by choosing a threshold intensity for the tracking point intensity.

To continuously track the marker in successive images, we pinpoint the tracker position manually for the first frame. We choose a rectangular region (**'search box'**) centered at this point and calculate a weighted mean for the '**estimated position**'(p) of tracker based on the pixel intensities. We shift the center of the search-box to the estimated position. Choosing an appropriately large searchbox and high enough frame rate, we can ensure that the tracker for the second frame lies within the search box. So, we can determine the new '**estimated position**'

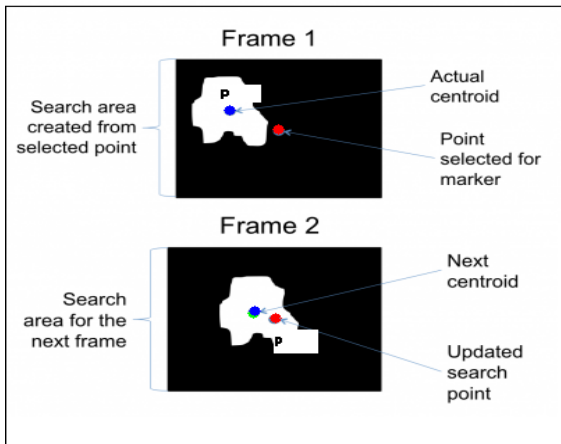


FIG. 10. Tracking using Matlab

of the tracker in the second frame using the same weighted mean method. We then update the center of the search-box to the estimated tracker position in the second frame. This process is repeated successively over all the images (fig 10).

Appendix C: Conversion from pixel to angular coordinates

One interesting observation is that the pendulum base vibrates with small amplitudes, even when the shaker is turned off. This is due to momentum transfer between the pendulum and the shaker. This does not

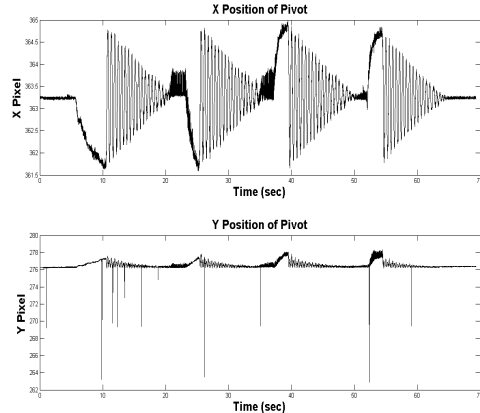


FIG. 11. Tracking pivot marker using labview

effect the motion drastically when the shaker is turned on, since the frequency of the shaker is large compared to that induced by pendulum. But it does give skewed information when the shaker is turned off, like in the spin-down experiment. The image below shows

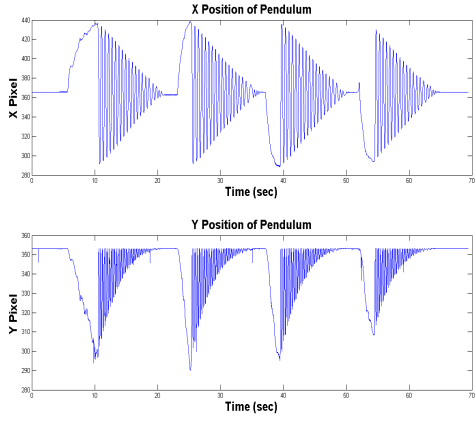


FIG. 12. Tracking pendulum marker using lab-view

the plot of tracked data of the pendulum (fig 12) and also the pivot (fig 11) (both in pixel units) as a function of time. At every instant of time, we determine the angular displacement of the pendulum by the following expression

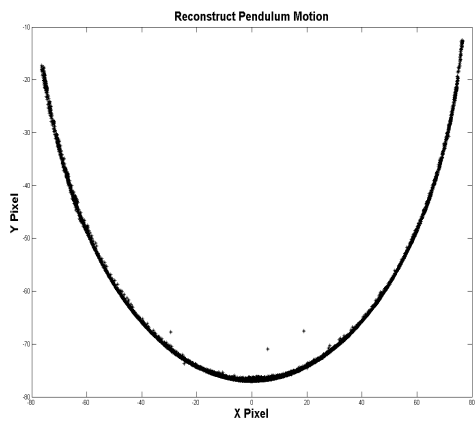


FIG. 13. Reconstructing pendulum motion

$$X_{pendulum,pivot} = X_{pendulum} - X_{pivot} \quad (C1)$$

$$Y_{pendulum,pivot} = Y_{pendulum} - Y_{pivot} \quad (C2)$$

$$\theta = -\tan^{-1}\left(\frac{X_{pen,piv}}{Y_{pen,piv}}\right) \quad (C3)$$

REFERENCES

- ¹N. G.-J. James A. Blackburn, H.J.T. Smith, “Stability and hopf bifurcation in an inverted pendulum,” Am. J. Phys **60** (1992).
- ²G. G. M. V. Bartuccelli and K. V. Georgiou, “On the dynamics of a vertically driven damped planar pendulum,” Proc. R. Soc. Lond. A **458**, 30073022 (2002).
- ³K. F. Chen, “Standing human - an inverted pendulum,” Lat. Am. J. Phys. Educ **2** (2008).
- ⁴I. D. Loram and M. Lakie, “Human balancing of an inverted pendulum: position control by small, ballistic-like, throw and catch movements,” Journal of Physiology **540**, 1111–1124 (2002).
- ⁵H. P. Kalmus, “The inverted pendulum,” Am. J. Phys **38**, 874–878 (1970).